RAYLEIGH WAVE ELLIPTICITY ESTIMATION FROM AMBIENT SEISMIC NOISE USING SINGLE AND MULTIPLE VECTOR-SENSOR TECHNIQUES

Manuel Hobiger[(1)], *Nicolas Le Bihan*[(2)], *Cécile Cornou*[(1)] *and Pierre-Yves Bard*[(1)]

(1): Laboratoire de Géophysique Interne et Tectonophysique, IRD: R157, LCPC, CNRS, Université Joseph Fourier, Maison des Géosciences, BP 53, 38041 Grenoble Cedex 9, France
phone: + (33) 4 76 63 52 25,
fax: + (33) 4 76 63 52 52,
email: manuel.hobiger@obs.ujf-grenoble.fr

(2): GIPSA-Lab, CNRS, 961, Rue de la Houille Blanche, BP 46, 38402 Grenoble Cedex, France
phone: + (33) 4 76 82 64 86,
fax: + (33) 4 76 57 47 90,
email: nicolas.le-bihan@gipsa-lab.inpg.fr

ABSTRACT

In this paper, we present three new methods to evaluate the ellipticity of polarized signals generated by seismic ambient vibrations. Classically, the estimation of Rayleigh wave ellipticity is performed using a spectrum ratio approach [15]. Here, we propose to use two single-sensor techniques (based on ellipse fitting [8] and random decrement [2]) and one multi-sensor technique (based on quaternion-MUSIC [12]) to substitute the existing algorithm. Rayleigh wave ellipticity is an important geophysical parameter because its estimation as a function of frequency leads to velocity vs. depth estimation, *i.e.* identification of the underground structure. We illustrate the three algorithms on simulation data and compare them to the existing approach.

1. INTRODUCTION

Geophysical signals carry information about the medium they have propagated through. In seismology it is common use to take advantage of the constant seismic activity to perform passive tomography [1]. The "ambient seismic noise" is indeed built of several types of waves. By analyzing them, conclusions about the medium characteristics can be drawn. In this paper, we are interested in surface waves called Rayleigh waves. In contrast to "classical" noise, these waves are polarized. The particle movement of Rayleigh waves describes an ellipse. The ratio of the horizontal axis to the vertical axis of the ellipse is called ellipticity. It is a function of frequency. In this paper, we focus on the estimation of the frequency dependency of Rayleigh wave ellipticity from passive recordings of ambient ground vibrations. In order to record polarization parameters, it is necessary to use vector-sensors whose outputs consist of three signals measuring displacements in three orthogonal directions of space.
In seismology, a standard way to access ellipticity is to use the spectral ratio between horizontal and vertical displacement measurements [3]. This way of doing has advantages in terms of simplicity but may not be very accurate as other wave types than Rayleigh waves also contribute to the wave field [4]. The P- and S-wave velocity profile (velocity as a function of depth) of the underground structure can be obtained by inversion of the ellipticity curve (ellipticity ε as a function of frequency ν, [5, 16]). Therefore, errors in the ellipticity curve lead to inaccurate estimation of the velocity profile of the underground structure.
In order to improve the estimation of ellipticity, we propose three different new methods: DELFI (Direct ellipse fitting for Rayleigh wave ellipticity estimation), RayDec (Rayleigh wave ellipticity estimation by using the random decrement technique) and MUSIQUE (MUSIC using quaternions for Rayleigh wave ellipticity estimation). DELFI and RayDec use single vector-sensors, MUSIQUE takes an array of multiple vector-sensors into account. The proposed techniques are compared and their limitations are given.

2. RAYLEIGH WAVE ELLIPTICITY IN SEISMOLOGY

First, we introduce the term of Rayleigh wave ellipticity as understood in seismology. After briefly recalling the underlying physics, we present the signals we will use to determine the ellipticity.

2.1 Surface waves and underground structure

Four main wave types are important in seismology. P- and S-waves represent pressure and shear body waves, respectively. Rayleigh and Love waves are surface waves, *i.e.* they propagate along the earth's surface. Their energy decreases as $1/r$ compared to $1/r^2$ for body waves where r is the distance to an earthquake hypocenter. Therefore surface waves are important for seismic hazard assessment.
Love waves are transverse waves which are confined to the surface layer. Rayleigh waves, which are also called "ground roll", are waves with a vertical and a horizontal component. The movement of a particle under the influence of a Rayleigh wave describes an ellipse in the plane formed by the vertical axis and the wave propagation direction. At the surface of homogeneous halfspaces, the movement of the fundamental mode is retrograde, *i.e.* the horizontal movement advances the vertical movement by $\pi/2$ in phase. Prograde movement corresponds to a phase difference of $-\pi/2$.
The underground structure of the earth's surface is in general not homogeneous but consists of different sedimentary layers superposing the bedrock. Every layer has different mechanical properties, *e.g.* P- and S-wave velocities. The properties of Rayleigh waves are closely related to the underground structure. An important polarization parameter of Rayleigh waves is the ellipticity ε. It is a function of frequency ν. Figure 1 shows a realistic model of the P- and S-wave velocity profile of an underground structure and the corresponding $\varepsilon(\nu)$-curve. Inversion techniques exist allowing the underground P- and S-wave velocity profiles to be derived from the $\varepsilon(\nu)$-curve of the Rayleigh waves [16].
The knowledge of the soil structure of a given site is important in order to estimate the ground motion and the associated risk for buildings in the case of an earthquake.

2.2 Sensors and arrays

In seismology, the earth's movements are recorded using vector-sensors called geophones. Such sensors are made of three co-located sensors recording the ground motion in three orthogonal directions. As a result, the output signal is a 3D vector-valued time-series. By convention, the three sensors are aligned in north-south, east-west and vertical direction.
A number of vector-sensors can be arranged to form an array. Thus, this configuration enables the measurement of the azimuth and velocity of incoming waves. In the following, the east-west signal of the vector-sensor will be denoted by $x(t)$, the north-south signal by $y(t)$ and the vertical signal by $z(t)$.

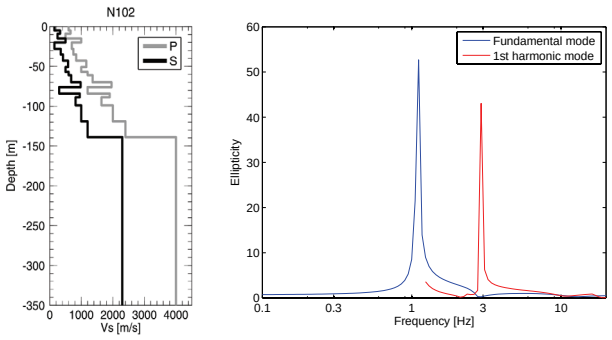

Figure 1: On the left, the used P- and S-wave velocity profile model. On the right, the theoretical frequency-ellipticity curve corresponding to this model for the fundamental and the first harmonic Rayleigh wave mode.

2.3 Existing technique: H/V spectrum ratios

A widespread approach to estimate ellipticity ε as a function of frequency ν for Rayleigh waves is the so-called H/V technique [15]. It is a single-sensor technique which consists of calculating the direct ratio between the horizontal and the vertical spectrum:

$$\varepsilon_{H/V}(\nu) = \frac{\sqrt{|X(\nu)|^2 + |Y(\nu)|^2}}{\sqrt{2}\,|Z(\nu)|}. \tag{1}$$

Note that for some frequencies, $|Z(\nu)|$ may vanish, which corresponds to singular points in the $\varepsilon(\nu)$ curve. In addition to Rayleigh waves, Love and body waves may also be recorded. As the movement of Love waves is restricted to the horizontal plane, the H/V approach systematically over-estimates ellipticity. Using assumptions on the proportion of Rayleigh and Love waves present in the wave field, it is possible to correct the over-estimation errors. However, there is no guarantee that the assumptions are in accordance with reality. This is a major source of error in the H/V approach. This motivates the search for other techniques for the estimation of $\varepsilon(\nu)$.

3. SINGLE-SENSOR APPROACH

In this section, we present two approaches to perform ellipticity estimation using the signal recorded on a single three-component vector-sensor. Their performances will be illustrated in Section 5.

3.1 Direct ellipse fitting (DELFI)

Consider the vector-valued signal $\vec{\mathbf{s}}(t)$ describing the movement of a soil particle in 3D space with time, given as $\vec{\mathbf{s}}(t) = [x(t)\ y(t)\ z(t)]^T$ taking values in $\mathbb{R}^3$. First, $\vec{\mathbf{s}}(t)$ is band-pass filtered around a frequency ν with bandwidth $d\nu$. Then, the following processing is performed independently for each frequency.

The filtered signal is cut in blocks of time length $T = 1/\nu$. The total length of the signal is assumed to be much longer than T. Each time-window consists thus of $N = T/dt$ samples where dt is the sampling period. The three-component signal of one time-window is noted $\mathbf{S}_w = [X_w\ Y_w\ Z_w]^T$ and is of dimension $3 \times N$. The polarization of Rayleigh waves is confined to a vertical plane, in opposition to the movement of noise signals which lie in 3D space. In order to project the signal $\mathbf{S}_w$ onto a vertical plane, we use the covariance matrix $\mathbf{C}_w$ built by the two horizontal components by $\mathbf{C}_w = [X_w\ Y_w]^T[X_w\ Y_w]$.

The Eigenvalue Decomposition (EVD) of $\mathbf{C}_w$ gives access to its eigenvalues λ_1 and λ_2 (ranked in increasing order, *i.e.* $\lambda_1 < \lambda_2$) and associated eigenvectors $\vec{\mathbf{u}}_1$ and $\vec{\mathbf{u}}_2$. The eigenvectors are normal vectors to two orthogonal vertical planes. The associated eigenvalues are the sums of the squared distances between the data points and the respective planes.

The 2D plane where the signal $\vec{\mathbf{s}}_w(t)$ is mostly confined is the one orthogonal to $\vec{\mathbf{u}}_1$ as it is associated to the smallest eigenvalue λ_1, *i.e.* the corresponding plane is spanned by the eigenvector $\vec{\mathbf{u}}_2$ and the vertical unit vector. The horizontal components of the time-window signal $\mathbf{S}_w$ are then projected onto an axis to build a horizontal signal H_w by $H_w = [X_w\ Y_w] \cdot \vec{\mathbf{u}}_2$. The 2D signal is then built by $\mathbf{S}'_w = [H_w\ Z_w]^T$.

Finally, the ellipticity measurement is performed using a modified version of the ellipse fitting algorithm proposed by *Fitzgibbon et al.* [8]. The modifications of the algorithm ensure that the axes of the ellipse are in horizontal and vertical directions. The algorithm yields the horizontal axis h_w, the vertical axis v_w and a parameter d_w^2 indicating the actual sum of squared distances between the data points and the fitted ellipse.

The ellipticity $\varepsilon(\nu)$ is calculated by averaging the found horizontal and vertical axes of all signal blocks for the corresponding frequency using the distance parameter d_w^2 as weighting factor:

$$\varepsilon_{DELFI}(\nu) = \frac{\sum h_w/d_w^2}{\sum v_w/d_w^2}. \tag{2}$$

The only free parameter of the method is $d\nu$.

3.2 Random decrement (RayDec)

The random decrement technique is commonly used to characterize dynamic parameters of buildings [7, 11]. It is classically applied to one-component (scalar valued) signals. We propose a three-component version of this technique in order to estimate $\varepsilon(\nu)$.

The following processing is performed independently for each frequency. First, the three components of $\vec{\mathbf{s}}(t)$ are filtered in a frequency range of bandwidth $d\nu$ around a central frequency ν. The filtered components are called $x_\nu(t)$, $y_\nu(t)$ and $z_\nu(t)$.

The next step is to search for the times τ_i where the signal sign changes from negative to positive on the vertical component ($z_\nu(\tau_i) \leq 0$, $z_\nu(\tau_i + dt) > 0$). For each of these τ_i a signal block of length Δ is stored on all three components. The number of buffered blocks thus depends on the analyzed signal itself. In order to compensate the natural $\pi/2$ phase shift, *i.e.* $1/(4\nu)$ in time, between the vertical and horizontal component signals of a Rayleigh wave, a phase shift is applied to x_ν and y_ν. The buffered signals then are:

$$\begin{cases} z_{\nu,b,i}(t) &= z_\nu(\tau_i + t) \\ x_{\nu,b,i}(t) &= x_\nu(\tau_i - \frac{1}{4\nu} + t), \\ y_{\nu,b,i}(t) &= y_\nu(\tau_i - \frac{1}{4\nu} + t). \end{cases} \tag{3}$$

for $0 \leq t \leq \Delta$. Index i specifies the change of sign position while index b stands for *buffered*. The east-west and north-south components, namely $x_{\nu,b,i}(t)$ and $y_{\nu,b,i}(t)$, of every buffered signal $\vec{\mathbf{s}}_{\nu,b,i}(t)$ are then projected onto a single axis to build a *horizontal component* in the following way:

$$h_{\nu,b,i}(t) = \sin\vartheta_i \cdot x_{\nu,b,i}(t) + \cos\vartheta_i \cdot y_{\nu,b,i}(t). \tag{4}$$

The azimuth angle ϑ_i is chosen to maximize the correlation $C(\vartheta_i) = \int_0^\Delta z_{\nu,b,i}(t) \cdot h_{\nu,b,i}(t)dt$ between the vertical signal $z_{\nu,b,i}(t)$ and the horizontal signal $h_{\nu,b,i}(t)$. The azimuth angle ϑ_i is thus obtained by

$$\vartheta_i = \tan^{-1}\left(\frac{\int_0^\Delta z_{\nu,b,i}(t) \cdot x_{\nu,b,i}(t)dt}{\int_0^\Delta z_{\nu,b,i}(t) \cdot y_{\nu,b,i}(t)dt}\right). \tag{5}$$

From the two possible $\vartheta_i \in [0^\circ, 360^\circ[$ satisfying equation (5) we choose the one leading to a positive correlation. At this point, the method does not distinguish between prograde and retrograde particle motion as prograde Rayleigh waves are treated as retrograde waves arriving from the opposite azimuth.

Although the angle ϑ_i maximizes the correlation, $z_{\nu,b,i}(t)$ and $h_{\nu,b,i}(t)$ can still be weakly correlated. Therefore, a correlation factor defined by

$$c_{\nu,b,i} = \frac{\int_0^\Delta z_{\nu,b,i}(t) \cdot h_{\nu,b,i}(t)dt}{\sqrt{\int_0^\Delta z^2_{\nu,b,i}(t)dt \cdot \int_0^\Delta h^2_{\nu,b,i}(t)dt}} \tag{6}$$

is used as weighting factor in the summation of the signals $z_{\nu,b,i}(t)$ and $h_{\nu,b,i}(t)$:

$$\begin{aligned} z_{\nu,s}(t) &= \sum_i c^2_{\nu,b,i} \cdot z_{\nu,b,i}(t) \\ h_{\nu,s}(t) &= \sum_i c^2_{\nu,b,i} \cdot h_{\nu,b,i}(t). \end{aligned} \tag{7}$$

Finally, the ellipticity is obtained by

$$\varepsilon_{RayDec}(\nu) = \sqrt{\frac{\int_0^\Delta h^2_{\nu,s}(t)dt}{\int_0^\Delta z^2_{\nu,s}(t)dt}}. \tag{8}$$

Repeated execution of this algorithm over the whole frequency range yields the frequency-ellipticity curve. The length of the buffered signal Δ and the width of the frequency filter $d\nu$ can be chosen arbitrarily.

4. MULTIPLE-SENSOR APPROACH (MUSIQUE)

In this section, we propose a way to take advantage of array measurements. The proposed approach is based on MUSIC algorithm and uses two of its versions: "classical" MUSIC to perform wave identification and "quaternion" MUSIC for ellipticity estimation. The array consists of N_S three-component sensors. The N_S time sample records are cut into blocks of $N_T = n_P/(\nu\ dt)$ data points each, where n_P is the number of periods corresponding to the frequency ν in the block and dt the sampling period. The cut time samples are stored in three $N_S \times N_T$ data matrices $\mathbf{S}_i(t)$ with $i = 1$ for *vertical*, $i = 2$ for *east* $-$ *west* and $i = 3$ for *north* $-$ *south* component. Fourier transform of these three data matrices yields the three matrices $\mathbf{S}_i(\nu)$ of dimensions $N_S \times N_T$.

4.1 First step: Azimuth estimation

The first step of our approach is to perform a "classical" MUSIC to identify the azimuth and velocity of an incoming wave. Note that this is a narrow-band MUSIC of bandwidth $d\nu$. Therefore, the *spectral matrix* is computed. Each one-component *spectral matrix* $\mathbf{M}_i(\nu) \in \mathbb{C}^{N_S \times N_S}$ is given by $\mathbf{M}_i(\nu) = \mathbf{S}_i(\nu)\mathbf{S}_i^\dagger(\nu)$. Then, the *total* sample covariance matrix $\mathbf{M}(\nu) \in \mathbb{C}^{N_S \times N_S}$ is obtained by $\mathbf{M}(\nu) = \sum_{i=1}^3 \mathbf{M}_i(\nu)$.
The N_{big} biggest eigenvalues of the matrix $\mathbf{M}(\nu)$ are identified to belong to the signal subspace and the other $(N_S - N_{big})$ to the noise subspace. It should be noted that due to the later performed projection into a plane the technique can only yield reliable results if the wave field is dominated by one wave and therefore $N_{big} = 1$. The noise subspace $\mathbf{G}(\nu) \in \mathbb{C}^{N_S \times (N_S - N_{big})}$ is hence built using the associated eigenvectors.
An incident Rayleigh wave with azimuth ϑ and phase velocity c is assumed. The associated wave vector is thus $\vec{\kappa}(\vartheta) = [-\sin\vartheta\ -\cos\vartheta\ 0]^T$ and the *time-delay vector* $\vec{\delta}(\nu,\vartheta,c) \in \mathbb{R}^{N_S \times 1}$ is given by

$$\vec{\delta}(\nu,\vartheta,c) = \frac{2\pi\nu}{c}\mathbf{R}\vec{\kappa}(\vartheta), \tag{9}$$

where $\mathbf{R} \in \mathbb{R}^{N_S \times 3}$ is the matrix of the positions of the array sensors and c the wave velocity. This leads to the steering vector $\vec{\gamma}(\nu,\vartheta,c) = \exp(-i\vec{\delta}(\nu,\vartheta,c))/\sqrt{N_S}$. The MUSIC functional $F(\nu,\vartheta,c)$ is finally given by:

$$F(\nu,\vartheta,c) = \frac{1}{\vec{\gamma}^\dagger(\nu,\vartheta,c)\mathbf{G}(\nu)\mathbf{G}^\dagger(\nu)\vec{\gamma}(\nu,\vartheta,c)}. \tag{10}$$

A grid search is performed in order to find the set of parameters (ϑ_0, c_0) maximizing this functional.
Now, as the movement of Rayleigh waves is confined to a plane spanned by the wave vector and the vertical axis, the original signals are projected into the vertical plane spanned by the wave vector just found. This means that the original vertical signal is left unchanged and the two horizontal signals are rotated using ϑ_0. The new signal $\mathbf{S}_p(t)$ consists of two matrices, $\mathbf{S}_{p1}(t)$ and $\mathbf{S}_{p2}(t)$, as it is confined to a 2D plane (instead of 3 components). It is obtained from the original signal by:

$$\begin{aligned} \mathbf{S}_{p1}(t) &= \mathbf{S}_1(t) \\ \mathbf{S}_{p2}(t) &= -\sin\vartheta_0 \cdot \mathbf{S}_2(t) - \cos\vartheta_0 \cdot \mathbf{S}_3(t). \end{aligned} \tag{11}$$

Fourier transforms of $\mathbf{S}_{p1}(t)$ and $\mathbf{S}_{p2}(t)$ give the matrices $\mathbf{S}_{p1}(\nu)$ and $\mathbf{S}_{p2}(\nu)$. Now that the signals are confined in the propagation plane of the Rayleigh wave, we can proceed to the estimation of ellipticity.

4.2 Second step: Ellipticity estimation

The second step of our approach consists in using a quaternion MUSIC algorithm to estimate the polarization parameters of the identified wave. *Miron et al.* [13] demonstrated its ability to perform polarization estimation. Therefore, we first build a quaternion valued data matrix $\mathbf{S}_q(\nu) \in \mathbb{H}^{N_S \times N_T}$ in the frequency domain [13]:

$$\begin{aligned} \mathbf{S}_q(\nu) &= \Re(\mathbf{S}_{p1}(\nu)) + \mathtt{i} \cdot \Re(\mathbf{S}_{p2}(\nu)) \\ &\quad + \mathtt{j} \cdot \Im(\mathbf{S}_{p1}(\nu)) + \mathtt{k} \cdot \Im(\mathbf{S}_{p2}(\nu)), \end{aligned} \tag{12}$$

where `i`, `j` and `k` are the three quaternion imaginary units [17]. The quaternion valued spectral matrix $\mathbf{M}_q(\nu)$ is given by $\mathbf{M}_q(\nu) = \mathbf{S}_q(\nu)\ \mathbf{S}_q^\dagger(\nu)$. Here again, the noise subspace $\mathbf{G}_q(\nu)$ is built by the $(N_S - N_{big})$ eigenvectors corresponding to the smallest eigenvalues, where N_{big} is the same number of sources as defined in the first step. In agreement with *Miron et al.* [13], the quaternion steering vector is given by:

$$\vec{\gamma}_q(\nu,\rho,\varphi) = [\cos(\rho) + \mathtt{i}\sin(\rho)e^{\mathtt{j}\varphi}]e^{-\mathtt{j}\vec{\delta}(\nu,\vartheta_0,c_0)}/\sqrt{N_S} \tag{13}$$

where ρ and φ are the polarization parameters of the wave and $\vec{\delta}(\nu,\vartheta_0,c_0)$ is the array delay vector given by equation (9) with $\vartheta = \vartheta_0$ and $c = c_0$. The ellipticity ε is the ratio of the amplitudes of horizontal and vertical motion, *i.e.*

$$\varepsilon_{MUSIQUE} = \sin\rho/\cos\rho = \tan\rho. \tag{14}$$

φ is the phase difference between the horizontal and the vertical signal. Note that we omitted the ν dependency of ρ and φ in eq. (13), but it should not be forgotten that their values depend on ν. A grid search yields the set of parameters (ρ_0, φ_0) that maximizes the quaternion MUSIC functional

$$\mathscr{F}_q(\nu,\rho,\varphi) = \frac{1}{\vec{\gamma}_q^\dagger(\nu,\rho,\varphi)\mathbf{G}_q(\nu)\mathbf{G}_q^\dagger(\nu)\vec{\gamma}_q(\nu,\rho,\varphi))} \tag{15}$$

Instead of using the parameter ρ to describe the ellipticity ε of the wave, it is possible to use ellipticity itself. However, as ellipticity values are in principle not limited, one would have to perform the parameter search for $0 \le \varepsilon \le \infty$. Therefore, it is advantageous to limit the search to $0 \le \rho \le \pi/2$ and to define ellipticity by equation (14). The phase difference φ is searched in the intervall $[0, 2\pi[$. For a retrograde Rayleigh wave, the phase difference will be found

around $\pi/2$, for a prograde Rayleigh wave it will be about $3\pi/2$.
The preceding processing is performed for every signal block of length N_T. For each frequency ν, the ellipticities of the signal blocks are averaged using the reciprocal value of the difference of φ from the the theoretical phase difference ($\pi/2$ for retrograde, $3\pi/2$ for prograde) and the signal energy of the signal block as weighting factors. In this way, the ellipticity curve $\varepsilon(\nu)$ is estimated.
The performances of the proposed multiple-sensor method are presented in the next section.

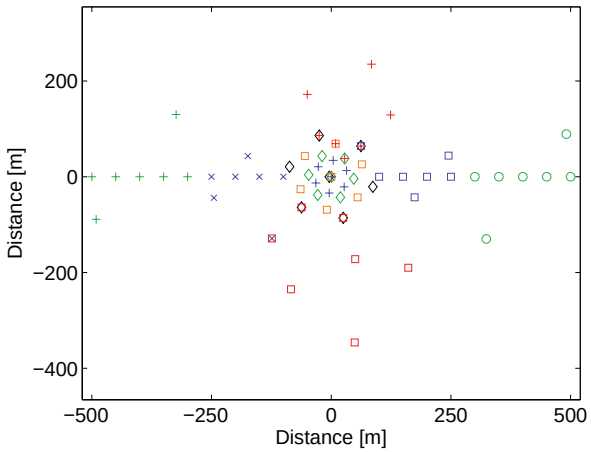

Figure 2: Layout of the sixty sensors forming ten seven-sensor arrays. Some stations belong to several arrays.

5. SIMULATION

In order to show the performances of the three proposed algorithms, we applied them to a set of synthetic seismic ambient vibrations. Model N102 of an international blind test benchmark [6] was used as underground structure. The P- and S-wave velocity profiles of the model, as well as the associated theoretical frequency-ellipticity curve, are shown in figure 1. 620 seconds of synthetic ambient vibrations were simulated as follows. Signal sources were modeled by forces with random orientation and amplitude located $0.5\,m$ below the surface [14]. The forces were distributed randomly in time and space. The time function of each source was a delta-like signal with a flat Fourier frequency-amplitude spectrum between 0.1 and $20\,Hz$. The associated wave field was computed by using the wavenumber-based technique of Hisada [9, 10] and contains all body and surface wave types. As the goal of this investigation is the Rayleigh wave ellipticity as a function of frequency, Love and body waves can be considered as "noise". However, the signal-to-noise ratio is unknown and the robustness of the methods under different signal-to-noise ratios cannot be investigated. As the signal generation mimics the generation of real seismic ambient vibrations this case can though be considered realistic.
The recordings were simulated for sixty seismic sensors. Their spatial distribution is shown in figure 2. The noise sources distribution covered all possible azimuths and distances up to around $1200\,m$ from the origin. Therefore, every seismic sensor represents a different set of data. As the underground structure is the same at every point of the model, the theoretical ellipticity is the same for each sensor. For H/V, DELFI and RayDec, the sixty sensors were used independently. To test MUSIQUE, ten arrays of seven sensors each were formed, some sensors belonging to several arrays. The Rayleigh wave ellipticity estimations of the three presented new methods and the classical H/V technique are shown in figure 3 in comparison to the theoretical ellipticity curve of the model.
The used free parameters are:
for DELFI, $d\nu = 0.2\nu$; for RayDec, $d\nu = 0.2\nu$ and $\Delta = 10/\nu$; for MUSIQUE, $d\nu = 0.2\nu$ and $n_P = 10$.

The H/V technique overestimates ellipticity considerably, especially at frequencies above and below the peak frequency. Compared to H/V, DELFI only improves the peak frequency estimation. As it works on the raw signals, it does not eliminate Love and body waves and therefore its results are close to H/V results. The RayDec curve is very close to the theoretical curve over the whole analyzed frequency range. RayDec is a statistical method which averages over a large number of time-windows to efficiently eliminate other wave types than Rayleigh waves. That is why its results are very close to the theoretical curve. For MUSIQUE, the results are in good agreement with theory over the whole frequency range, but compared to RayDec, the error bars are larger. However, MUSIQUE does not suppress Love and body waves but also shows good results in identifying ellipticity. As the curve is the average for ten arrays, its results could propably be better with more arrays or more signal analysed. Optimisation of the array layouts (array aperture and geometry) could also improve the results.
In testing the methods, we have stated that RayDec requires a minimum signal length of some minutes to give stable results. DELFI and MUSIQUE, in contrast, do not require a minimum signal length and are thus applicable to non-stationary wave trains as produced in earthquakes. As MUSIQUE uses array measurements, it also gives an estimate of the azimuth and wave velocity. Therefore, it is also possible to distinguish between prograde and retrograde Rayleigh wave movement. DELFI and RayDec do not give the wave velocity and give two possible azimuths. Therefore, they cannot distinguish between prograde and retrograde Rayleigh waves.

6. CONCLUSION

The three new methods have been succesfully applied to synthetic noise data and have proven their ability to estimate the frequency-ellipticity curves of Rayleigh waves. The further work is to quantify the differences between the results of the method and the theory and to test the methods on other simulation data. Completing those tasks would validate the applicability of the proposed methods to real seismic data.

ACKNOWLEDGMENTS

Noise synthetics were performed at the Service Commun de Calcul Intensif (SCCI) of Grenoble observatory, France (OSUG). This work is supported by the NERIES European project and the ANR QSHA project.

REFERENCES

[1] Aki, K., *Space and time spectra of stationary stochastic waves, with special reference to microtremors*, Bull. Earthq. Res. Inst. 35, pp. 415-456, 1957.

[2] Asmussen, J. C., *Modal analysis based on the random decrement technique*, PhD thesis, University of Aalborg, 1997.

[3] Bard, P.-Y., *Microtremor measurements: a tool for site effect estimation?*, State-of-the-art paper, Second International Symposium on the Effects of Surface Geology on seismic motion, Yokohama, December 1-3, 1998, Irikura, Kudo, Okada & Sasatani (eds), Balkema, 3, pp. 1251-1279, 1999.

[4] Bonnefoy-Claudet, S., Köhler, A., Cornou, C., Wathelet, M., and Bard, P.-Y., *Effects of Love Waves on Microtremor H/V Ratio*, Bull. Seism. Soc. Am., Vol. 98, pp. 288-300, 2008.

[5] Boore, D. M., and Toksöz, M. N., *Rayleigh wave particle motion and crustal structure*, Bull. Seism. Soc. Am., Vol. 59, pp. 331-346, 1969.

[6] Cornou, C., Ohrnberger, M., Boore, D. M., Kudo, K., and Bard, P.-Y., *Using ambient noise array techniques for site characterisation: results from an international benchmark*, Proc. 3rd Int. Symp. on the Effects of Surface Geology on Seismic Motion, Grenoble, 30 August - 01 September, 2006, 92 pages, LCPC Editions, 2009, in press.

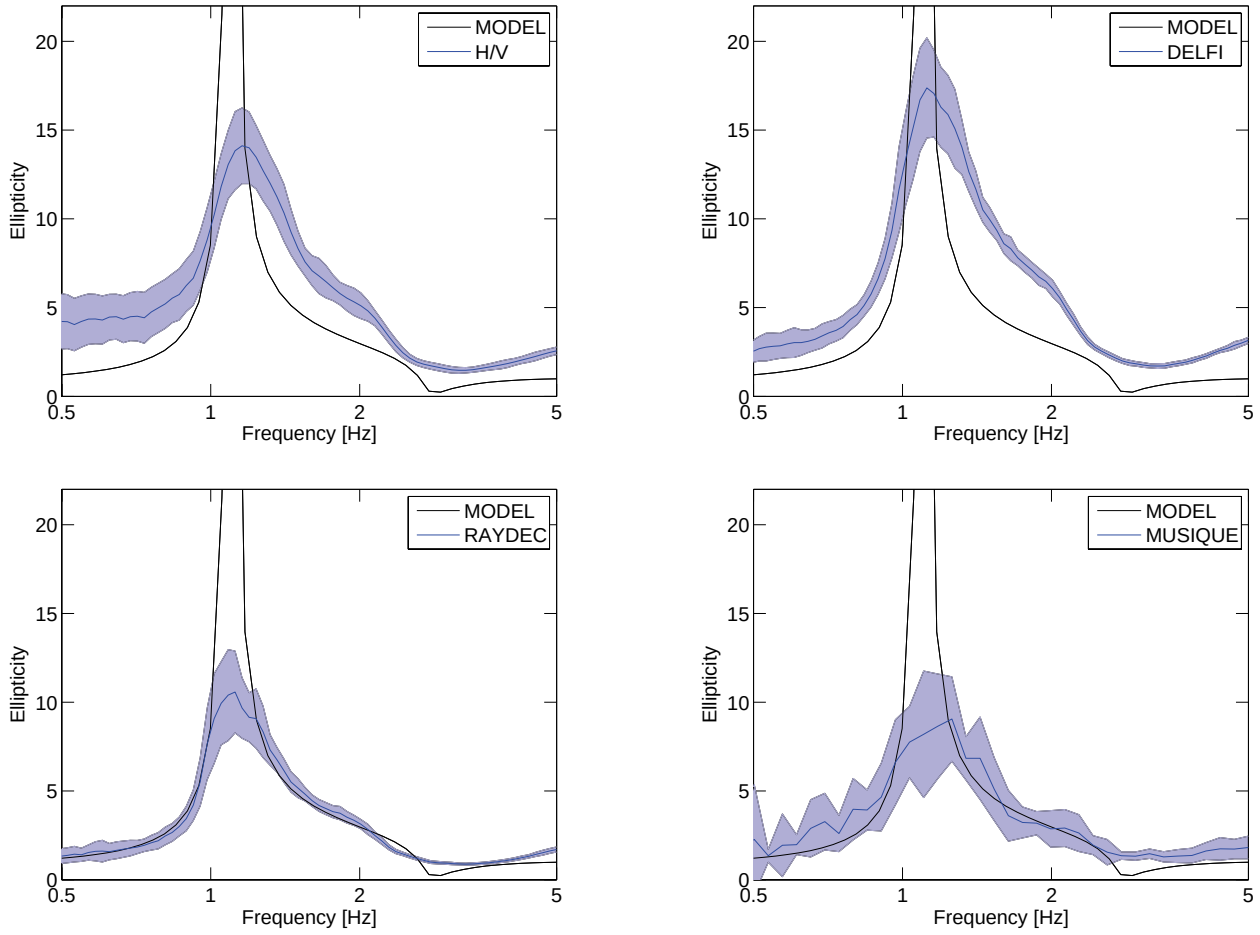

Figure 3: Rayleigh wave ellipticity curves obtained by analyzing 620 seconds of synthetic seismic ambient vibrations by H/V, DELFI, RayDec and MUSIQUE techniques in comparison to the theoretical ellipticity curve of the model. For H/V, DELFI and RayDec, the average curves of 60 sensors are shown with the corresponding error range. For MUSIQUE, the average curve with error margin for ten arrays is shown.

[7] Dunand, F., *Pertinence du bruit de fond sismique pour la caractérisation dynamique et l'aide au diagnostic sismique des structures de génie civil*, PhD thesis, Université Joseph Fourier Grenoble, 2005.

[8] Fitzgibbon, M., Pilu, A. W., and Fisher, R. B., *Direct least square fitting of ellipses*, IEEE Transactions on Pattern Analysis and Machine Intelligence, Vol. 21, No. 5, pp. 476-480, 1999.

[9] Hisada, Y., *An efficient method for computing Green's functions for a layered halfspace with sources and receivers at close depths*, Bull. Seism. Soc. Am., Vol. 84, pp. 1456-1472, 1994.

[10] Hisada, Y., *An efficient method for computing Green's functions for a layered halfspace with sources and receivers at close depths (Part 2)*, Bull. Seism. Soc. Am., Vol. 85, pp. 1080-1093, 1995.

[11] Michel, C., Guéguen, P., and Bard, P.-Y., *Dynamic parameters of structures extracted from ambient vibration measurements: An aid for the seismic vulnerability assessment of existing buildings in moderate seismic hazard regions*, Soil Dynamics and Earthquake Engineering, 28, pp. 593-604, 2008.

[12] Miron, S., Le Bihan, N., and Mars, J. I., *High resolution vector-sensor array processing using quaternions*, IEEE International Conference on Statistical Signal Processing, Bordeaux, France, 2005.

[13] Miron, S., Le Bihan, N., and Mars, J. I., *Quaternion-MUSIC for vector-sensor array processing*, IEEE Transactions on Signal Processing, Vol. 54, No. 4, pp. 1218-1229, 2006.

[14] Moczo, P. and Kristek, J., *FD code to generate noise synthetics*, Sesame report D02.09, available at http://SESAME-FP5.obs.ujf-grenoble.fr

[15] Nakamura, Y. *A method for dynamic characteristics estimation of subsurface using microtremors on the ground surface*, Quarterly reports of the Railway Technical Research Institute Tokyo, 30, pp. 2533. 1989.

[16] Arai, H., and Tokimatsu, K., *S-Wave velocity profiling by inversion of microtremor H/V spectrum*, Bull. Seism. Soc. Am., Vol. 94, pp. 53-63, 2004.

[17] Ward, J. P., Quaternions and Cayley Numbers, Algebra and applications, Kluwer Academic, 1997.